# Distinguishing transient from persistent tactile agnosia after partial anterior circulation infarcts - Behavioral and neuroimaging evidence for white matter disconnection

**John H. Missimer, Eugenio Abela, Manuela Pastore-Wapp, Roland Wiest, Bruno J. Weder**

Supplementary Material

- Tactile Object Recognition task
- Principal component analysis of behavioral data
- Mahalanobis distances and Gaussian cluster model
- Proportional overlaps of white matter tracts with lesions
- Tractotron results concerning white matter tract lesions using BCBtoolkit
- The interrelation between anterior arcuate fasciculus and SLF III – a classification issue

**Tactile Object Recognition task**

Table S1: Objects used for tactile object recognition task

| | | | | | |
|---|---|---|---|---|---|
| Marble | Clothes peg | Nutshell | Tape reel | Thimble | Eraser |
| Pencil | Button | Coin | Key | Battery | Ring |
| Sharpener | Glue stick | Tippex | Wooden plug | Bottle opener | Screw |
| Paperclip | Velcro | Pebble | Rubber band | Dice | Nail |
| Hook | Ball pen | Block battery | Shim | Syringe (5 ml) | Key ring |

**Principal component analysis of behavioral data**

Table S2. Patient data used in principal component analysis expressed as z-scores

| patient | age | lesvol | NIH 0 | PSO 0 | MAC 0 | MIC 0 | PPT 0 | TOR 0 | TOR 9 |
|---|---|---|---|---|---|---|---|---|---|
| RTI1 | 0.6200 | 0.4653 | 6 | 13.48 | -14.3 | -22.30 | -18.60 | -57.20 | -15.20 |
| RTI2 | 1.0396 | 1.1997 | 4 | 6.77 | -21.00 | -19.40 | -113.40 | -59.20 | -11.20 |
| RTI3 | 1.2074 | 1.9091 | 5 | 4.17 | -39.30 | -33.70 | -48.10 | -59.20 | -9.20 |
| RTI4 | -1.2261 | -0.1321 | 4 | 58.82 | -6.00 | -2.30 | -0.70 | -37.20 | -21.20 |
| RTI5 | 0.7879 | 0.0173 | 3 | 14.40 | -22.70 | -33.70 | -58.30 | -35.20 | 0.80 |
| RTI6 | 0.7879 | 2.0585 | 4 | 27.60 | -16.00 | -10.90 | -34.20 | -51.20 | -9.20 |
| RTI7 | 1.3752 | -0.4744 | 3 | 9.12 | -9.30 | -5.10 | -8.40 | -19.20 | -9.20 |
| PTI1 | -1.0582 | 2.0585 | 6 | 20.1 | -19.30 | -15.10 | -26.30 | -59.20 | -59.20 |
| PTI2 | -0.8065 | 16.2601 | 14 | 51.28 | -14.30 | -33.70 | -100.20 | -59.20 | -59.20 |
| PTI3 | -0.9743 | 0.9072 | 6 | 27.56 | -39.30 | -33.70 | -112.40 | -59.20 | -39.20 |
| PTI4 | 0.3683 | 2.9298 | 6 | 5.85 | -39.30 | -33.70 | -112.40 | -59.20 | -39.20 |
| PTI5 | -1.3939 | 4.5105 | 3 | 5.35 | -39.30 | -33.70 | -48.10 | -59.20 | -39.20 |
| PTI6 | 0.1165 | 0.6832 | 11 | 38.87 | -14.30 | -33.70 | -100.20 | -53.20 | -55.20 |
| PTI7 | -1.0582 | 1.3864 | 11 | 22.70 | -39.30 | -33.70 | -19.60 | -59.20 | -53.20 |

Table S3. Relevant features of PCA comprising PSO 0, MAC 0 and TOR 0. Corr coef are the correlation coefficients of TOR 9 with the patient scores, and p the corresponding probabilities.

| | % explained | Corr coef | p |
|---|---|---|---|
| PC1 | 62 | -0.12 | 0.69 |
| PC2 | 30 | 0.67 | 0.008 |

Table S4. Patient scores for PC2 of PCA comprising PSO 0, MAC 0 and TOR 0. These are plotted in Figure 1.

| recovered | PC1 | PC2 | permanent | PC1 | PC2 |
|---|---|---|---|---|---|
| RTI1 | -3.23 | 3.79 | PTI1 | -1.02 | -3.01 |
| RTI2 | -12.69 | 3.06 | PTI2 | 26.82 | -16.83 |
| RTI3 | -24.35 | -2.64 | PTI3 | -5.42 | -14.44 |
| RTI4 | 43.18 | -0.43 | PTI4 | -22.99 | -3.48 |
| RTI5 | -0.95 | 17.13 | PTI5 | -23.40 | -3.23 |
| RTI6 | 8.93 | 0.66 | PTI6 | 18.40 | -5.92 |
| RTI7 | 6.09 | 37.31 | PTI7 | -9.36 | -11.98 |

Table S5. The component expression coefficients describing the PC patterns

| | PSO 0 | MAC 0 | TOR 0 |
|---|---|---|---|
| PC1 | 0.8093 | 0.5221 | 0.2693 |
| PC2 | -0.5046 | 0.3831 | 0.7737 |

Table S6. Kruskal-Wallis ANOVA of PC2: RTI vs PTI

| Source | SS | df | MS | $\chi 2$ | $p > \chi 2$ |
|---|---|---|---|---|---|
| Columns | 171.5 | 1 | 171.5 | 9.8 | 0.0017 |
| Error | 56 | 12 | 4.667 | | |
| total | 227.5 | 13 | | | |

Figure S1. Scatter plot of PC patient scores: PC2 vs PC1 for PTI (red) and RTI (blue).

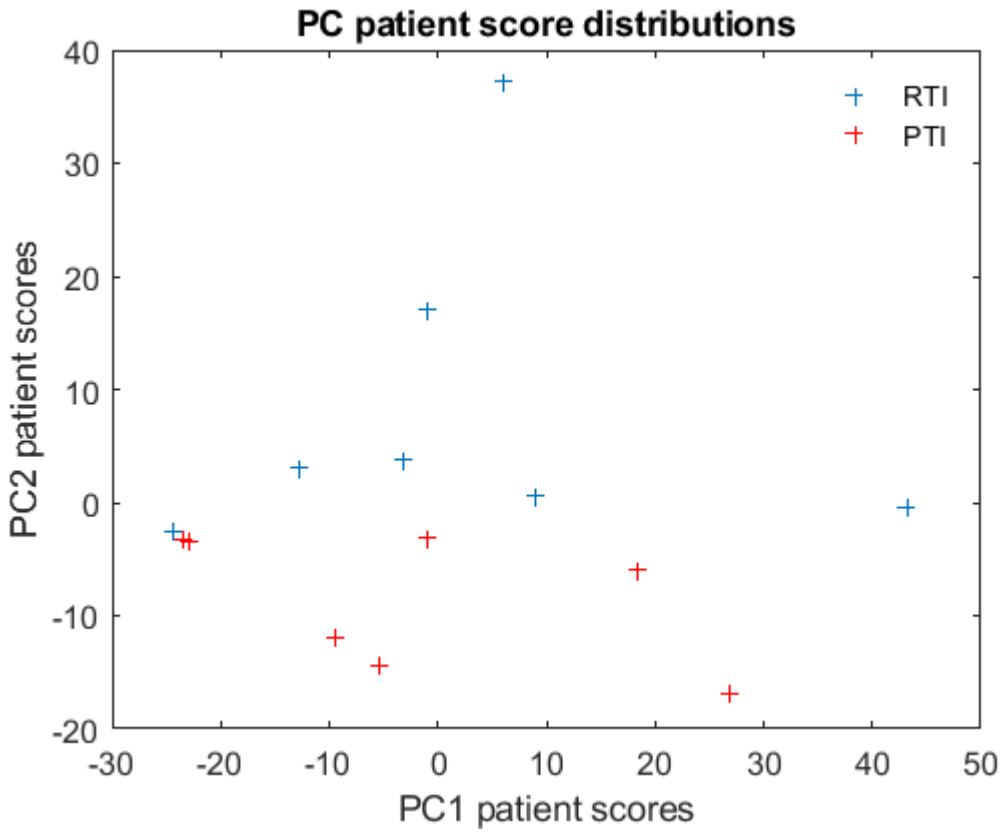

## Mahalanobis distances and Gaussian mixing model

Table S6. Mahalanobis distances derived from PSO 9, MAC 9 and TOR 9 with respect to unimpaired patients at nine months and Gaussian mixture modeling

| recovered | dist | permanent | dist |
|---|---|---|---|
| RTI1 | 179 | PTI1 | 3004 |
| RTI2 | 183 | PTI2 | 3004 |
| RTI3 | 542 | PTI3 | 1862 |
| RTI4 | 355 | PTI4 | 1919 |
| RTI5 | 16 | PTI5 | 2038 |
| RTI6 | 147 | PTI6 | 3530 |
| RTI7 | 93 | PTI7 | 2382 |

Table S7. Gaussian mixing model derived from Mahalanobis distances of Table S5. With 21 iterations, the distribution with 3 component in 1 dimension yielded a log-likelihood of -192.3

| Component | Mixing Proportion | Mean | Sigma |
|---|---|---|---|
| 1 TN | 0.544 | 1.551 | 1.94 |
| 2 RTI | 0.261 | 163.220 | 165.87 |
| 3 PTI | 0.195 | 2592.2 | 685.42 |

Figure S2. Histogram of Mahalanobis distances with Gaussians derived from the mixing model. The Gaussians have been rescaled to accommodate the histograms, but the relative heights of the Gaussians are correct. Green denotes TN; Blue denotes RTI; red PTI.

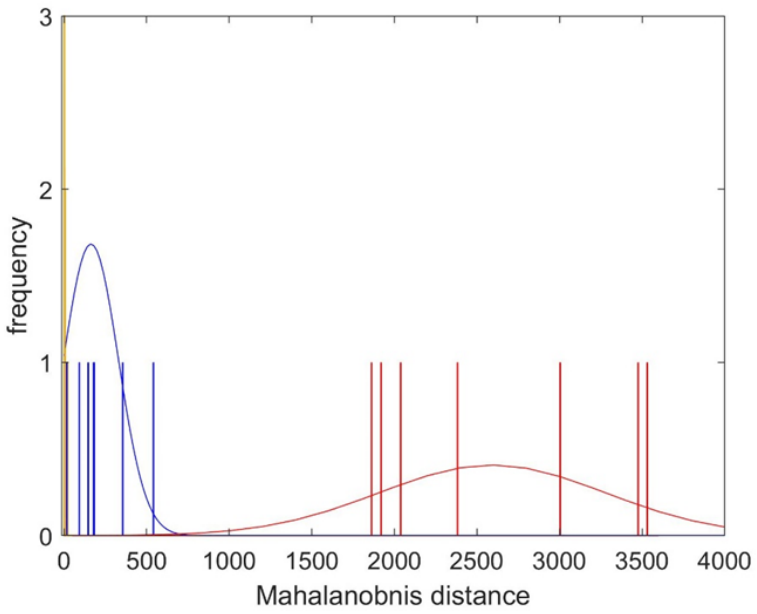

## Proportional overlaps of white matter tract segments with lesions

Table S8. Proportions of overlap of lesion with white matter tract for patient subgroups used in Table 3 of manuscript.

| | Anterior Arcuate Fasciculus AH | Superior Longitudinal Fasciculus III AH | Corpus_callosum |
|---|---|---|---|
| RTI1 | 0.597 | 0.395 | 0.056 |
| RTI2 | 0.415 | 0.341 | 0.038 |
| RTI3 | 0.562 | 0.487 | 0.075 |
| RTI4 | 0.046 | 0.042 | 0.029 |
| RTI5 | 0.159 | 0.125 | 0.007 |
| RTI6 | 0.101 | 0.091 | 0.038 |
| RTI7 | 0.005 | 0.002 | 0.009 |
| PTI1 | 0.529 | 0.433 | 0.071 |
| PTI2 | 0.993 | 0.942 | 0.169 |
| PTI3 | 0.726 | 0.309 | 0.033 |
| PTI4 | 0.770 | 0.514 | 0.052 |
| PTI5 | 0.446 | 0.437 | 0.074 |
| PTI6 | 0.846 | 0.669 | 0.116 |
| PTI7 | 0.434 | 0.341 | 0.030 |

Supplementary Material

Table S9. Tractotron results (Foulon et al. 2018; http://www.toolkit.bcblab.com) showing probability (P) and mean proportion of overlap (OL) of lesion projection into white matter tracts of PTI, RTI and TN subgroups. The threshold P>0.5 indicates disconnection of a specific tract due to the lesion. AH denotes affected hand.

| **PTI subgroup** | **Mean_P** | **Mean_OL** | **SD_OL** | **RTI subgroup** | **Mean_P** | **Mean_OL** | **SD_OL** |
|---|---|---|---|---|---|---|---|
| Anterior Arcuate Fasciculus AH | 1.00 | 0.68 | 0.21 | Superior_Longitudinal_Fasciculus_II_AH | 1.00 | 0.20 | 0.11 |
| Corpus_callosum | 1.00 | 0.08 | 0.05 | Cortico_Spinal_AH | 0.99 | 0.14 | 0.07 |
| Superior_Longitudinal_Fasciculus_III_AH | 1.00 | 0.52 | 0.22 | Fronto_Striatal_AH | 0.96 | 0.06 | 0.03 |
| Superior_Longitudinal_Fasciculus_II_AH | 1.00 | 0.38 | 0.21 | Handinf_U_tract_AH | 0.96 | 0.45 | 0.26 |
| Fronto_Insular_tract5_AH | 0.99 | 0.78 | 0.29 | Anterior Arcuate Fasciculus_AH | 0.95 | 0.27 | 0.25 |
| Handinf_U_tract_AH | 0.97 | 0.72 | 0.29 | Pons_AH | 0.95 | 0.10 | 0.05 |
| Arcuate_Long_Segment_AH | 0.96 | 0.51 | 0.32 | Corpus_callosum | 0.94 | 0.04 | 0.02 |
| Arcuate_Posterior_Segment_AH | 0.95 | 0.51 | 0.39 | Superior_Longitudinal_Fasciculus_III_AH | 0.94 | 0.21 | 0.19 |
| Cortico_Spinal_AH | 0.92 | 0.12 | 0.11 | Arcuate_Long_Segment_AH | 0.92 | 0.20 | 0.15 |
| Fronto_Striatal_AH | 0.88 | 0.07 | 0.08 | Frontal_Commissural | 0.88 | 0.02 | 0.02 |
| Fronto_Insular_tract4_AH | 0.90 | 0.63 | 0.36 | Anterior_Thalamic_Projections_AH | 0.85 | 0.03 | 0.02 |
| Superior_Longitudinal_Fasciculus_I_AH | 0.88 | 0.06 | 0.06 | Superior_Longitudinal_Fasciculus_I_AH | 0.85 | 0.08 | 0.07 |
| Frontal_Aslant_tract_AH | 0.88 | 0.20 | 0.20 | Handsup_U_tract_AH | 0.80 | 0.24 | 0.21 |
| Frontal_Commissural | 0.87 | 0.03 | 0.03 | Frontal_Aslant_tract_AH | 0.80 | 0.04 | 0.03 |
| Inferior_Fronto_Occipital_fasciculus_AH | 0.86 | 0.07 | 0.13 | Frontal_Superior_Longitudinal_AH | 0.75 | 0.09 | 0.10 |
| Handsup_U_tract_AH | 0.85 | 0.34 | 0.21 | Fronto_Insular_tract5_AH | 0.75 | 0.47 | 0.46 |
| Pons_AH | 0.81 | 0.07 | 0.08 | Handmid_U_tract_AH | 0.64 | 0.37 | 0.36 |
| Face_U_tract_AH | 0.82 | 0.84 | 0.27 | Cingulum | 0.62 | 0.02 | 0.03 |
| Frontal_Superior_Longitudinal_AH | 0.81 | 0.06 | 0.06 | Fronto_Insular_tract4_AH | 0.59 | 0.28 | 0.34 |
| Inferior_Longitudinal_AH | 0.83 | 0.09 | 0.11 | Face_U_tract_AH | 0.53 | 0.32 | 0.37 |
| Handmid_U_tract_AH | 0.77 | 0.38 | 0.37 | Frontal_Inferior_Longitudinal_AH | 0.53 | 0.02 | 0.03 |
| Frontal_Inferior_Longitudinal_AH | 0.75 | 0.34 | 0.41 | Arcuate_Posterior_ Fasciculus _AH | 0.50 | 0.08 | 0.12 |
| Anterior_Thalamic_Projections_AH | 0.74 | 0.04 | 0.06 | | | | |
| Fronto_Insular_tract3_AH | 0.74 | 0.40 | 0.41 | | | | |
| Optic_Radiations_AH | 0.62 | 0.05 | 0.08 | | | | |
| | | | | | | | |

Supplementary Material

| NT subgroup | Mean_P | Mean_OL | SD_OL |
|---|---|---|---|
| Superior_Longitudinal_Fasciculus_II_AH | 0.99 | 0.11 | 0.07 |
| Corpus_callosum | 0.99 | 0.02 | 0.02 |
| Pons_AH | 0.93 | 0.07 | 0.06 |
| Fronto_Striatal_AH | 0.93 | 0.04 | 0.04 |
| Cortico_Spinal_AH | 0.90 | 0.08 | 0.08 |
| Superior_Longitudinal_Fasciculus_I_AH | 0.90 | 0.04 | 0.06 |
| Handsup_U_tract_AH | 0.89 | 0.21 | 0.17 |
| Frontal_Commissural | 0.89 | 0.03 | 0.03 |
| Anterior_Thalamic_Projections_AH | 0.87 | 0.02 | 0.03 |
| Handinf_U_tract_AH | 0.86 | 0.19 | 0.21 |
| Superior_Longitudinal_Fasciculus_III_AH | 0.84 | 0.09 | 0.13 |
| Frontal_Superior_Longitudinal_AH | 0.81 | 0.07 | 0.12 |
| Anterior Arcuate Fasciculus_AH | 0.72 | 0.10 | 0.15 |
| Frontal_Aslant_tract_AH | 0.70 | 0.04 | 0.07 |
| Arcuate_Long_Segment_AH | 0.70 | 0.11 | 0.21 |
| Handmid_U_tract_AH | 0.62 | 0.14 | 0.20 |

## The interrelation between anterior arcuate fasciculus and SLF III – a classification issue

Figure S3. Interweaving of ROIs, representing horizontal segments of the anterior arcuate fascicle and SLF III, illustrates the difficulty of differentiating between them at the macroscopic level. The white area in figure represents the anterior arcuate fasciculus, the red border marks SLF III and pale yellow to yellow varying degrees of intersection. The green areas show subareas of angular gyrus, parakeet subarea PGa and green pear subarea PGp. It becomes evident that SLF III extends more anteriorly and posteriorly to the posterior supramarginal gyrus and angular gyrus.